articles

molecular pharmaceutics

pH-Induced Nanosegregation of Ritonavir to Lyotropic Liquid Crystal of Higher Solubility than Crystalline Polymorphs

Barbara Rodríguez-Spong,[‡] Alison Acciacca,[‡] David Fleisher,[†] and Naír Rodríguez-Hornedo*

Department of Pharmaceutical Sciences, University of Michigan, 428 Church Street, Ann Arbor, Michigan 48109-1065

Received July 30, 2008; Revised Manuscript Received October 14, 2008; Accepted October 14, 2008

Abstract: Birefringent spherical vesicles of ritonavir (RTV) are formed by increasing the pH of aqueous solutions from 1 to 3 or to 7 and by addition of water to ethanol solutions at room temperature. Increasing the pH creates supersaturation levels of 30−400. Upon this change in pH, the solutions become translucent, implying that some kind of RTV assembly was formed. Small spherical vesicles of narrow size distribution are detectable only after a few hours by optical microscopy. The vesicles show similar X-ray diffraction patterns and differential scanning calorimetry (DSC) behavior to amorphous RTV prepared by melt-quenching crystalline RTV. Examination by polarized optical microscopy suggests that these are lyotropic liquid crystalline (LLC) assemblies. Small-angle X-ray scattering and synchrotron X-ray diffraction further support the presence of orientational order that is associated with a nematic structure. RTV self-organizes into various phases as a result of the supersaturation created in aqueous solutions. The LLC vesicles do not fuse but slowly transform to the polymorphs of RTV (in days), Form I and finally Form II. Amorphous RTV in aqueous suspension also undergoes a transformation to a mesophase of similar morphology. Transformation pathways are consistent with measured dissolution rates and solubilities: amorphous > LLC ≫ Form I > Form II. The dissolution and solubility of LLC is slightly lower than that of the amorphous phase and about 20 times higher than that of Form II. RTV also self-assembles at the air/water interface as indicated by the decrease in surface tension of aqueous solutions. This behavior is similar to that of amphiphilic molecules that induce LLC formation.

Keywords: Mesophases; liquid crystals; precipitation

Introduction

Approximately 50% of all pharmaceuticals are weakly acidic or basic compounds.[1] For those compounds with pK_a values in the range of physiologic pH, variations in ionization state following drug administration can impact drug delivery by influencing membrane permeability or aqueous solubility. The oral administration of high dose, low pK_a weak base drugs may be of special concern. Drugs in this class may be highly soluble when ionized in the acidic environment of the stomach but may become supersaturated in the more alkaline environment of the small intestine due to lower solubility of the un-ionized form. This raises the potential for the compound to precipitate and may limit the fraction of drug that is bioavailable. This fundamental oral delivery problem is typically overlooked and not fully understood. Knowledge of the crystallization pathways for these compounds is essential in order to optimize dissolution rate and avoid precipitation of an undesired form during GI transit.

Precipitation pathways and rates are a function not only of physiological pH but also of supersaturation. A highly

* To whom correspondence should be addressed. Mailing address: Department of Pharmaceutical Sciences, 428 Church Street, Ann Arbor, MI 48109-1065. Telephone: 734-763-0101. Fax: 734-615-6162. E-mail: nrh@umich.edu.

† In memory of David Fleisher.

‡ Present address: Pfizer Inc., Groton, CT, 06340.

(1) Stahl, P. H.; Wermuth, C. G. *Handbook of Pharmaceutical Salts: Properties, Selection and Use*; Wiley VCH: New York, 2002.

10.1021/mp800114k CCC: $40.75
Published on Web 10/31/2008

supersaturated solution may nucleate at a fast rate, potentially resulting in nano- or submicrometer crystalline, amorphous, or soft phases with different degrees of order and mobility, whereas low supersaturation will have a slower rate of precipitation, larger particles, and more stable phases. Supersaturation is a necessary and not a sufficient condition for precipitation and in some cases may not lead to nucleation and growth in the time scale of observation. Therefore, factors such as pH which influence supersaturation will have direct effects on nucleation and crystal growth rates, crystal morphology, and precipitation pathways.[2−4]

The human immunodeficiency virus (HIV) protease inhibitors are an example of high dose, low pK_a weakly basic drugs that exhibit pH-dependent solubility. This class of structurally related peptidomimetic compounds possesses moderate molecular size and high intrinsic lipophilicity, which, in itself, presents oral formulation challenges. Two drugs in this class, ritonavir and saquinivir, have been developed as self-emulsifying or microemulsion-based lipidic formulations to overcome poor aqueous solubility and improve oral delivery.[5,6] It has been noted that only limited information is available in the literature regarding the solubility of these drugs in buffered solutions[7] or their potential for precipitation under physiologically relevant conditions.

Indinavir (Crixivan) is one HIV protease inhibitor for which the development of nephrolithiasis and crystalluria in patients has been reported, demonstrating the potential for weakly basic drugs to exhibit pH-dependent crystallization in vivo.[8] Kopp, et al.[8] found that crystals of indinavir were present in starburst forms and irregular plate forms in the urine of patients. The precipitation of indinavir was also studied at different concentrations and pH values in synthetic urine. Consistent with the pH-solubility profile of this weak base, crystallization induction times were notably shorter at urinary pH values above 6.0 and delayed at lower pH values.[9] The potential for indinavir precipitation during gastric emptying has also been discussed in the literature. *In vitro* crystallization models were compared with clinical observations of reduced indinavir oral bioavailability in humans following elevations in gastric pH.[10,11] Indinavir precipitates when supersaturation is created by raising solution pH to 7 and crystallization induction times are shortened by the presence of formulation excipients or crystal seeds.[11]

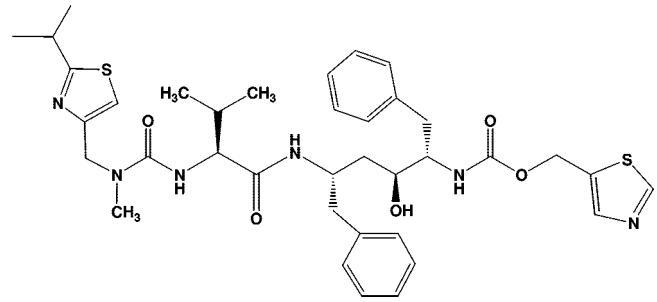

Figure 1. Chemical structure of ritonavir.

Ritonavir (RTV), shown in Figure 1, is another weakly basic HIV protease inhibitor which exhibits a marked pH-dependent solubility profile. Polymorphic behavior of RTV was discovered following the appearance of a new, less soluble polymorph (Form II) that dictated market withdrawal of the original hydroalcoholic solution-containing capsule formulation (Norvir).[12,13] The potential for pH-induced crystallization from aqueous solutions has not been previously studied.

RTV has two thiazole groups with pK_a values of 1.8 and 2.6 and would exist as a dicationic species in the acidic environment of the stomach and as the free base at alkaline pH.[14] The aqueous solubility of RTV polymorphic Form I at pH 1.0, 37 °C is 400 μg/mL and drops to 1 μg/mL at pH 6.8.[14] The pH-solubility profile for this form is shown in

(2) Zipp, G. L.; Rodríguez-Hornedo, N. Growth mechanism and morphology of phenytoin and their relationship with crystallographic structure. *J. Phys. D: Appl. Phys.* **1993**, *26* (8B), B48−B55.

(3) Zipp, G. L.; Rodríguez-Hornedo, N. The mechanism of phenytoin crystal growth. *Int. J. Pharm.* **1993**, *98* (1−3), 189–201.

(4) Heimbach, T.; Oh, D.; Li, L. Y.; Rodríguez-Hornedo, N.; Garcia, G.; Fleisher, D. Enzyme-mediated precipitation of parent drugs from their phosphate prodrugs. *Int. J. Pharm.* **2003**, *261*, 81–92.

(5) Porter, C. J. H.; Charman, W. N. In vitro assessment of oral lipid based formulations. *Adv. Drug Delivery Rev.* **2001**, *50*, S127−S147.

(6) Gursoy, R. N.; Benita, S. Self-emulsifying drug delivery systems (SEDDS) for improved oral delivery of lipophilic drugs. *Biomed. Pharmacother.* **2004**, *58* (3), 173–182.

(7) Weiss, J.; Burhenne, J.; Riedel, K. D.; Haefeli, W. E. Poor solubility limiting significance of in-vitro studies with HIV protease inhibitors. *AIDS* **2002**, *16* (4), 674–676.

(8) Kopp, J. B.; Miller, K. D.; Mican, J. A. M.; Feuerstein, I. M.; Vaughan, E.; Baker, C.; Pannell, L. K.; Falloon, J. Crystalluria and urinary tract abnormalities associated with indinavir. *Ann. Intern. Med.* **1997**, *127* (2), 119–125.

(9) Grases, F.; Costa-Bauza, A.; Garcia-Gonzalez, R.; Payeras, A.; Bassa, A.; Torres, J. J.; Conte, A. Indinavir crystallization and urolithiasis. *Int. Urol. Nephrol.* **1999**, *31* (1), 23–29.

(10) Carver, P. L.; Fleisher, D.; Zhou, S. Y.; Kaul, D.; Kazanjian, P.; Li, C. Meal composition effects on the oral bioavailability of indinavir in HIV-infected patients. *Pharm. Res.* **1999**, *16* (5), 718–724.

(11) Li, L. Y.; Rodríguez-Hornedo, N.; Heimbach, T.; Fleisher, D. In-vitro crystallization of indinavir in the presence of ritonavir and as a function of pH. *J. Pharm. Pharmacol.* **2003**, *55* (5), 707–711.

(12) Bauer, J.; Spanton, S.; Henry, R.; Quick, J.; Dziki, W.; Porter, W.; Morris, J. Ritonavir: An extraordinary example of conformational polymorphism. *Pharm. Res.* **2001**, *18* (6), 859–866.

(13) Chemburkar, S. R.; Bauer, J.; Deming, K.; Spiwek, H.; Patel, K.; Morris, J.; Henry, R.; Spanton, S.; Dziki, W.; Porter, W.; Quick, J.; Bauer, P.; Donaubauer, J.; Narayanan, B. A.; Soldani, M.; Riley, D.; McFarland, K. Dealing with the impact of ritonavir polymorphs on the late stages of bulk drug process development. *Org. Process Res. Dev.* **2000**, *4* (5), 413–417.

(14) Law, D.; Krill, S. L.; Schmitt, E. A.; Fort, J. J.; Qiu, Y. H.; Wang, W. L.; Porter, W. R. Physicochemical considerations in the preparation of amorphous ritonavir-poly(ethylene glycol) 8000 solid dispersions. *J. Pharm. Sci.* **2001**, *90* (8), 1015–1025.

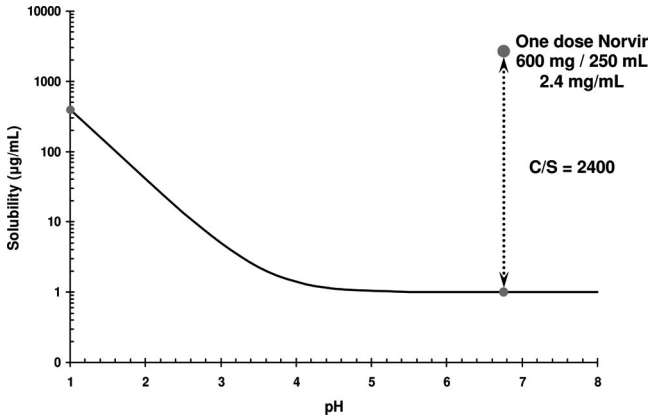

Figure 2. Calculated pH-solubility profile for ritonavir Form I at 37 °C according to the Henderson−Hasselbalch equation and reported solubilities at pH 1.0 and 6.8. (Krill et al.[14]).

Figure 2. On the basis of this profile, a single dose of Norvir (600 mg) taken with 8 oz (∼250 mL) of water could lead to supersaturations as high as 2400-fold in the small intestine. This supersaturated state is based on calculations of dilution of the liquid formulations of RTV and presents a sizable driving force for the precipitation of RTV, which is the primary focus of this report.

The purpose of this research is thus to examine the pH induced precipitation of RTV from aqueous solutions and to determine the crystallization pathways from aqueous solutions and from amorphous phases. Since changes in molecular assemblies that lead to different supramolecular architectures such as amorphous, liquid crystalline, and crystalline solids can alter physicochemical and pharmaceutical properties, the stability, solubility, and dissolution of RTV phases were also investigated.

Materials and Experimental Methods

Materials. RTV Form I and Form II were a gift from Abbott Laboratories (North Chicago, IL). Amorphous RTV was prepared by heating either crystalline phase to 135 °C (above the melting point) in an oil bath followed by rapid cooling in liquid nitrogen.[14] The amorphous solid was equilibrated to room temperature over anhydrous phosphorus pentoxide under vacuum in a desiccator to reduce the potential for moisture uptake and was then characterized by XRPD and DSC.

Water used in this study was filtered through a double deionized purification system (Milli Q Plus Water System, Millipore Co., Bedford, MA). Phosphoric acid, hydrochloric acid, and sodium hydroxide were ACS reagent grade and purchased from Sigma (St. Louis, MO). Anhydrous ethyl alcohol (200 proof) was USP grade and was purchased from Pharmco (Brookfield, CT).

Precipitation from Solution. pH-Induced Precipitation. Precipitation of RTV was induced at 22 °C by changing the pH of 0.3 M phosphoric acid solutions with RTV concentrations between 0.03 and 0.4 mg/g from pH 1 to 3 or 7 by addition of 1 M sodium hydroxide with constant stirring. Reaction scale volumes ranged from 50 μL to 15 mL. Solutions became translucent instantaneously and were transferred into Petri dishes. RTV phases were monitored while suspended in the precipitation medium by polarized optical microscopy and Raman spectroscopy as described below. The precipitate was harvested by vacuum filtration, rinsed with a saturated aqueous solution of RTV to remove any residual salts, and dried at room temperature (22−23 °C) under reduced pressure (25 mmHg) on Whatman #50 filter paper (Maidstone, England) for 30 min.

Precipitation from Ethanol. RTV was precipitated from ethanol solutions where supersaturation was created by the addition of 40−90% (w/w) water to RTV solutions of concentrations ranging from 0.5 to 78.5 mg/g at 22 °C with constant stirring. Phase transformations were studied by methods described above.

Chemical Analysis. Liquid chromatography mass spectrometry (LC-MS) was used to measure the chemical integrity of RTV solid phases before and after precipitation. High-performance liquid chromatography (HPLC) was performed using a Waters HPLC system (Waters, Inc., Milford, MA), with two Waters pumps (model 515), a Waters autosampler (WISP model 712), and a Waters UV detector (996 photodiode array detector). An Xterra C-18 reversed-phase column (5 μm, 4.6 × 250 mm) was used with the solvent system 0.1% trifluoroacetic acid (TFA) in water/0.1% TFA in acetonitrile by a gradient method of 0−40% organic component in 45 min. Molecular weights were confirmed by mass spectrometry using an ESI-MS Thermoquest LCQ electrospray ionization mass spectrometer.

Microscopy. The appearance and morphology of RTV phases was examined during precipitation and phase transformation studies while suspended in aqueous or ethanol solutions at room temperature (22−23 °C) using an inverted optical microscope (Nikon, Diaphot-TMD, Melville, NY) with 10× and 40× Nomarski objectives. Birefringence was observed using polarized optical microscopy (POM) (Leica, DMPL, Bannockburn, IL). A full wave plate filter was used in conjunction with crossed polarizers to enhance the optical features of some of the samples for image collection. Images were collected with a Spot Insight FireWire 4 Megasample Color Mosaic camera controlled with Spot software (Diagnostics Inc., Sterling Heights, MI).

The thermal behavior of the RTV precipitate was studied using a Leica DMPL polarizing optical microscope and a Linkham THMS600 hot stage with liquid nitrogen cooling (Linkham, U.K.). Films of the RTV precipitate obtained with a change in pH were grown on glass coverslips. The films were rinsed with a saturated aqueous solution of RTV to remove residual salt, covered by another glass coverslip, and observed by POM as the hot stage provided variable temperature analysis from −20 to 70 °C at rates of 2−10 °C/min. A full wave plate filter was used in conjunction with crossed polarizers to enhance the optical features of some of the samples for image collection. Images were collected with a Spot Insight FireWire 4 Megasample Color Mosaic camera controlled with Spot software.

Differential Scanning Calorimetry (DSC). Thermal behavior was determined by DSC using a Perkin-Elmer DSC-7 instrument (Wellesley, MA). Samples of approximately 5−10 mg were weighed into aluminum DSC pans, crimped with a pinhole lid, and heated at rates of 10 °C/min for crystalline samples and 20 °C/min for amorphous RTV under a dry nitrogen purge (20 cc/min). Thermal data are the average of three measurements. A two point calibration was performed with indium and zinc for high temperatures (156.6−419.5 °C) or *n*-dodecane and indium for subambient temperatures (−9.6 to 156.6 °C).

Modulated-DSC was performed using a DSC 2910 modulated DSC instrument (TA Instruments, New Castle, DE) with a refrigerated cooling system (RCS) attached. Samples of approximately 5 mg were weighed into aluminum DSC pans, crimped with a pinhole lid, and heated at a rate of 3 °C/min. A dry nitrogen purge was used at a flow rate of 50 cc/min through the DSC cell and 110 cc/min through the RCS. The system was calibrated with indium and *n*-dodecane, and heat capacity was calibrated using sapphire.

Thermal Gravimetric Analysis (TGA). The water/solvent content in solid phases of RTV was determined using a Perkin-Elmer TGA-7 instrument (Wellesley, MA). Samples of approximately 10 mg were placed in a platinum pan and heated at 10 °C/min under a dry nitrogen purge (20 cc/min).

X-ray Powder Diffraction (XRPD). Powder diffraction patterns of RTV solid phases were recorded using a Scintag X-ray diffractometer (Franklin, MA) using Cu Kα radiation ($\lambda = 1.54$Å), a tube voltage of 40 kV, and a tube current of 20 mA. The intensities were measured at 2θ values from 2° to 45° at a continuous scan rate of 2 °/min.

Synchrotron X-ray Powder Diffraction. Synchrotron analysis was performed at the Stanford Synchrotron Radiation Laboratory (SSRL, Stanford, CA). The high-resolution powder diffraction beamline 2-1 was used with the wavelength fixed at 1.240 Å, an electron energy of 3 GeV, and a current of 100−60 mA at an incident energy of 10 keV. Intensities were measured at 2θ values from 4° to 60°.

Small-Angle X-ray Scattering (SAXS). Small-angle X-ray scattering was used to measure diffraction peaks at low 2θ angles below 5° to identify long-range order inherent to the solid phase of RTV precipitated by change in pH. SAXS was performed using a Rigaku (Danvers, MA) 12 kW diffractometer equipped with a Kratky camera and a Braun 10 cm position sensitive detector. The scan rate was 0.12°/min from 0.2° to 3.5° 2θ. Radiation was generated from a Cu source at a wavelength of 1.542 Å.

Raman Spectroscopy. Raman spectra of solid phases were collected on a Renishaw Raman microscope (Hoffman Estates, IL) equipped with a Leica optical microscope and 785 nm laser. Samples were placed on aluminum covered slides for analysis. Five acquisitions of 10 s exposure time were averaged over a wavenumber range of 3600−200 cm^{-1} at a resolution of 1 cm^{-1}.

Equilibrium Solubility Measurement. The equilibrium solubility of RTV Form II was determined from undersaturation by adding excess solid phase to 0.1 M hydrochloric acid (pH 1). The suspensions were equilibrated in 250 mL jacketed beakers maintained at 25.0 ± 0.5 °C by a circulating temperature bath (Neslab, Portsmouth, NH), with constant stirring provided by an overhead stirrer. Equilibration was monitored for at least 48 h, as determined by UV/VIS spectroscopy (Beckman DU-650, Fullerton, CA). Samples were drawn at various time intervals using a 3 mL syringe and filtered using a 0.22 μm nylon filter (Millipore, Billerica, MA), allowing at least 2 mL to saturate the filter prior to sample collection. Each sample was diluted with water and analyzed by UV/VIS spectroscopy at a wavelength of 245 nm. Solubility studies were done in triplicate, and the solid phases at equilibrium were characterized by XRPD, DSC, and TGA.

Disk Dissolution Measurement. Intrinsic dissolution rates of RTV crystalline Forms I and II, amorphous RTV, and the solid phase precipitated by change in pH were measured from the initial concentration−time profile. The surface area of each solid was kept constant during dissolution by compressing each phase in a Wood's die of 10 mm diameter. Samples were compressed in the die using a Carver hydraulic press (Wabash, IN) by applying 1000 psi for 1 min. Compressed samples were analyzed by XRPD to confirm that a phase transformation had not occurred under the force of compression. The die containing the compacted sample was rotated at 100 rpm while suspended in 200 mL of 0.1 M HCl (pH 1) in a jacketed beaker maintained at 25.0 ± 0.5 °C by a circulating temperature bath (Neslab RTE-210, Portsmouth, NH). Solution concentrations were measured at 30 s intervals over 1 h by continuously circulating the dissolution medium with a peristaltic pump (Masterflex, Cole-Palmer, Niles, IL) through a 1 cm quartz cell inside a UV/VIS spectrophotometer (Perkin-Elmer Lambda 3B, Wellesley, MA) at 245 nm. Sink conditions were maintained throughout the experiment.

Surface Tension Measurements. RTV self-association at the air/water interface was studied from measurement of surface tension at 25.0 ± 0.5 °C by the Wilhelmy plate method using a platinum plate (Rosano surface tensiometer, Laboratory Products, Inc., Boston, MA). Solution temperature was controlled by a circulating water bath (Neslab RTE-210, Portsmouth, NH). The instrument was calibrated with known weights and by comparing the surface tension of water to reported values. Solutions consisted of 0.1 N HCl (pH 1) and 0.2 M phosphate buffer solutions adjusted to pH 3 and 7 using 0.1 N NaOH and RTV concentrations in the range of 0−0.455 mM (0.33 mg/mL), representing concentrations at saturation levels achieved in these solutions. All reported values are the average of five measurements.

Results

pH-Induced Precipitation. Aqueous solutions of RTV supersaturated by change in pH from 1 to 3 or to 7 instantaneously precipitate at initial supersaturation $(C/S)_i > 30$ at room temperature (22−23 °C). Solutions become translucent at a pH value of about 1.8, which is

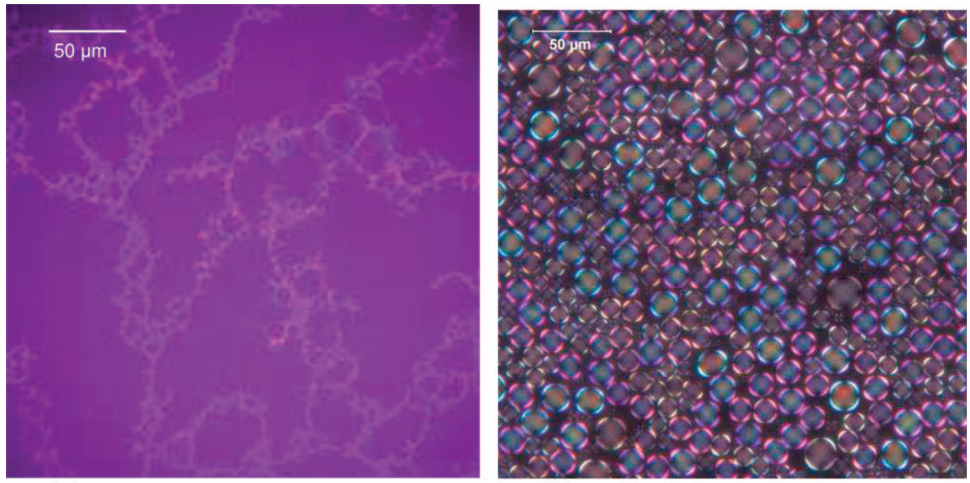

Figure 3. Precipitation of ritonavir at pH 3, $(C/S)_i = 400$ at 22 °C, as (a) an iridescent film at the air/water interface ($t = 30$ min) and (b) birefringent spherical vesicles ($t = 24$ h).

the pK_{a1} of RTV. The precipitated phase is below the level of detection by optical microscopy; however, as it grows, two different assemblies are detected. The first is an iridescent surface film having a very mobile, threadlike texture at the air/water interface (Figure 3a). The second is a phase of isolated small spherical vesicles suspended in solution (Figure 3b) and is detected by POM a few hours after translucence is detected. These vesicles are birefringent, display a very narrow size distribution, and do not further aggregate. The morphology and birefringence of vesicles suggests the formation of nanostructures with a level of mobility and order characteristic of mesophases and lyotropic liquid crystalline phases.[15−19]

The spherical vesicles (Figure 4a) remain in suspension for 1 day at room temperature before transforming to the Form I crystal polymorph of RTV (Figure 4b,c). Within 2 weeks, Form I transforms to Form II (Figure 4d), the most thermodynamically stable polymorph of RTV. The chemical integrity of each solid phase was confirmed by LC-MS, since acidic and basic environments have the potential for chemical degradation. The vesicles, when harvested from suspension by vacuum filtration, are stable when stored over anhydrous calcium sulfate at 5 °C and maintain a small degree of birefringence.

Precipitation of the mesophase was also induced by addition of water to ethanol solutions of RTV at 25 °C, and the crystallization pathways were similar to those induced by a change in pH (results not shown).

Characterization of Mesophase. Thermal Behavior. Thermal analysis by conventional and modulated DSC exhibits a second-order transition for the mesophase precipitated at pH 3 and 7 that is similar to that observed for the amorphous solid. The mesophase exhibits a glass transition (T_g) with an enthalpic peak (Figure 5). The enthalpic peak results from the method of preparation, since instantaneous precipitation through pH change may leave the system with some degree of molecular mobility as it relaxes to its equilibrium structure.[20−23] This enthalpic relaxation can be deconvoluted using modulated DSC to separate reversing and nonreversing thermal events, seen in Figure 6. As expected, the enthalpic peak is nonreversing and the T_g is resolved. The onset T_g of the mesophase structures (obtained at pH 3 and 7) and the onset T_g of amorphous RTV are not significantly different (48 °C). However, the difference between these phases is evident from the change in heat capacity at T_g, since $\Delta Cp_{amorphous} < \Delta Cp_{mesophase}$, 0.35 and 0.54 (Figure 6).

The structural changes inherent to the mesophase of RTV become evident when thermal behavior is visualized using

(15) Kuang, G.; Ji, Y.; Jia, X.; Li, Y.; Chen, E.; Wei, Y. Self-Assembly of Amino-Acid-Based Dendrons: Organogels and Lyotropic and Thermotropic Liquid Crystals. *Chem. Mater.* **2008**, *20*, 4173–4175.

(16) Chen, B.; Zheng, X.; Baumeister, U.; Ungar, G.; Tschierske, C. Liquid crystalline networks composed of pentagonal, square, and triangular cylinders. *Science* **2005**, *307*, 96–99.

(17) Kato, T.; Norihiro, N.; Kishimoto, K. Functional liquid-crystalline asemblies: self-organized soft materials. *Angew. Chem., Int. Ed.* **2006**, *45*, 38–68.

(18) Lechuga-Ballesteros, D.; Abdul-Fattah, A.; Stevenson, C. L.; Bennett, D. B. Properties and stability of a liquid crystal form of cyclosporine - The first reported naturally occurring peptide that exists as a thermotropic liquid crystal. *J. Pharm. Sci.* **2003**, *92* (9), 1821–1831.

(19) Horváth-Szabó, G.; Czarnecki, J.; Masliyah, J. Liquid crystals in aqueous solutions of sodium naphthenates. *J. Colloid Interface Sci.* **2001**, *236*, 233–241.

(20) Crowley, K. J.; Zografi, G. The use of thermal methods for predicting glass-former fragility. *Thermochim. Acta* **2001**, *380*, 79–93.

(21) Zhou, D.; Zhang, G. G. Z.; Law, D.; Grant, D. J. W.; Schmitt, E. A. Physical stability of amorphous pharmaceuticals: importance of configurational thermodynamic quantities and molecular mobility. *J. Pharm. Sci.* **2002**, *91* (8), 1863–1872.

(22) Hancock, B.; Shamblin, S. Molecular mobility of amorphous pharmaceuticals deretmined using differential scanning calorimetry. *Thermochim. Acta* **2001**, *380*, 95–107.

(23) Ediger, M. D.; Angell, C. A.; Nagel, S. R. Supercooled liquids and glasses. *J. Chem. Phys.* **1996**, *100* (31), 13200–13212.

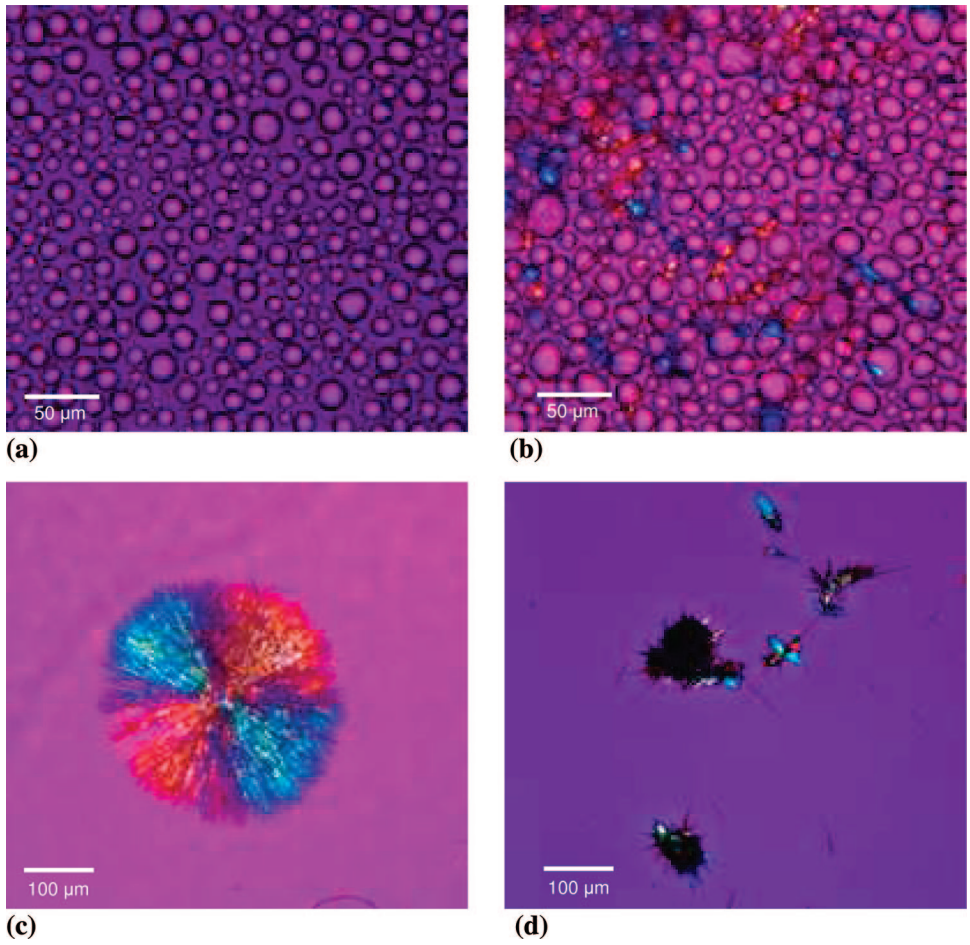

Figure 4. Phase transformation of ritonavir in suspension following precipitation at pH 3, $(C/S)_i = 400$ at 22 °C: (a) spherical vesicles at $t = 24$ h, (b) transformation of mesophase to Form I crystals at $t = 3$ days, (c) formation of starburst crystals of Form I after mesophase is depleted, $t = 5$ days, and (d) transformation to crystals of Form II at $t = 14$ days.

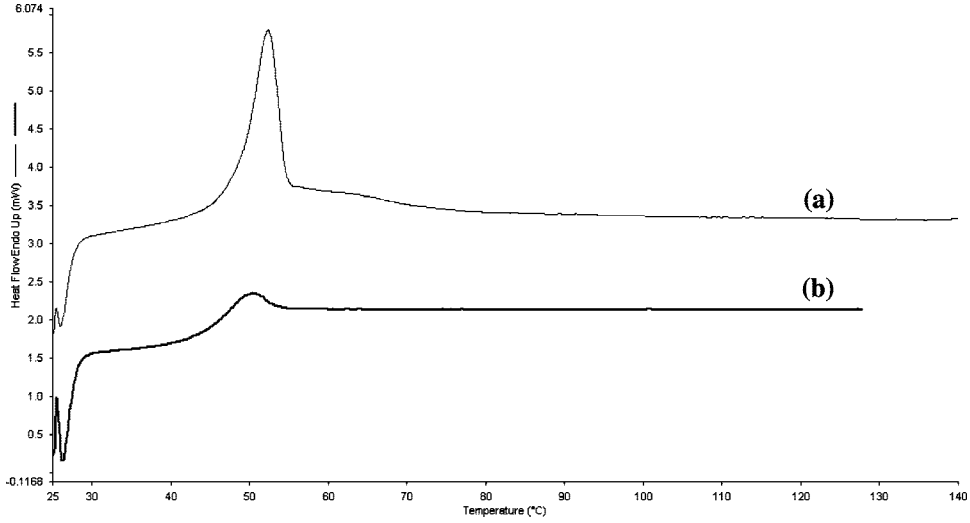

Figure 5. Conventional DSC scans for (a) mesophase precipitated at pH 3 and (b) amorphous ritonavir prepared by quench cooling the melt.

hot stage microscopy. The mesophase vesicles are birefringent, even when heated through the T_g (from −20 to 50 °C), suggesting that a level of long-range order is maintained throughout this temperature range (Figure 7a,b). At temperatures above the T_g (50−70 °C), the morphology changes as the mesophase vesicles coalesce and birefringence is lost

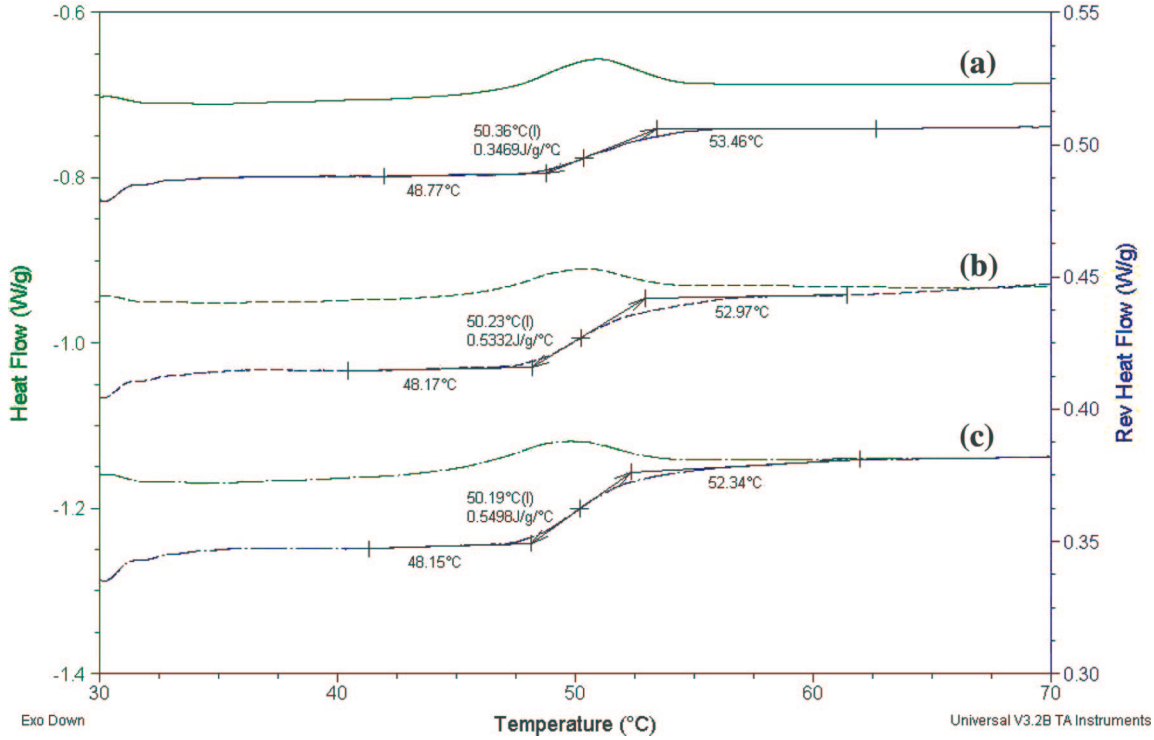

Figure 6. Modulated DSC scans showing similar glass transition temperatures of (a) amorphous ritonavir, (b) mesophase precipitated at pH 3, and (c) mesophase precipitated at pH 7. Heating rate = 3 °C/min.

(Figure 7d). Prior to this, the dehydration of the mesophase is observed as the vesicles swell and become porous at temperatures between 30 and 50 °C (Figure 7c). Therefore, the molecular mobility observed as an enthalpic relaxation by conventional DSC (Figure 5a) is associated with the morphological changes seen with increasing temperature by hot stage microscopy.

Raman Spectroscopy. Raman spectra could be used to distinguish the crystalline phases of RTV (Form I and II) from the disordered phases (amorphous and mesophase) (Figure 8). In particular, the crystalline phases can be readily identified based on differences in their supramolecular structures and molecular interactions. However, the spectra for the amorphous phase and mesophase are poorly resolved in comparison to the crystalline forms. Similar observations have been made in the past comparing the crystalline and amorphous phases of nifedipine, indomethacin, tolbutamide, and lacidipine[24] that have been related to the difference between an ordered and disordered structure. Furthermore, the spectra comparing the amorphous and mesophase structures are not significantly different. Infrared spectroscopy also failed to resolve the differences between these phases (data not shown). These results suggest that molecular level interactions in both phases are comparable. In fact, crystalline polymorphs having very similar hydrogen bonding patterns are often difficult to distinguish based on IR and Raman spectra alone.[25]

X-ray Diffraction. Similar to the Raman spectra of the mesophase, XRPD was unable to distinguish between amorphous RTV and the mesophase (Figure 9). The two crystalline polymorphs (Form I and II), however, have characteristic diffraction peaks at 3.32 and 6.75° for Form I and 9.51, 9.88, and 22.25° for Form II. The pH-induced mesophase does not exhibit characteristic powder diffraction peaks, and instead a halo with two diffuse peaks at low 2θ values is detected. The absence of sharp diffraction peaks by XRPD for the mesophase confirms a lack of three-dimensional long-range order.

Synchrotron X-ray diffraction patterns comparing the pH 3 mesophase, amorphous RTV, and crystalline Form II are shown in Figure 10. The crystallinity of Form II is evident from the diffraction peaks. The amorphous RTV shows an attenuation of peaks with an increase in 2θ, and the pH 3 mesophase shows an increase in intensity of a broad peak. This is indicative of a lack of long-range order.

Small-angle X-ray scattering results are shown in Figure 11. The evolution of diffraction pattern was detected as a function of time as the mesophase precipitated from solution ($(C/S)_i = 400$, pH 3, 22 °C) and grew over 23 h. No sharp peaks were observed, which would be indicative of long-range positional order. Birefringence combined with a lack of SAXS peaks is consistent with a nematic structure, which has orientational order but no positional order.

Surface Tension. The self-assembly of RTV in solutions and associated surface activity were determined by measuring

(24) Forster, A.; Hempenstall, J.; Rades, T. Characterization of glass solutions of poorly water-soluble drugs produced by melt extrusion with hydrophilic amorphous polymers. *J. Pharm. Pharmacol.* **2001**, *53* (3), 303–315.

(25) Colthup, N. B.; Daly, L. H.; Wiberley, S. E. *Introduction to Infrared and Raman Spectroscopy*; Academic Press, Inc.: San Diego, 1990.

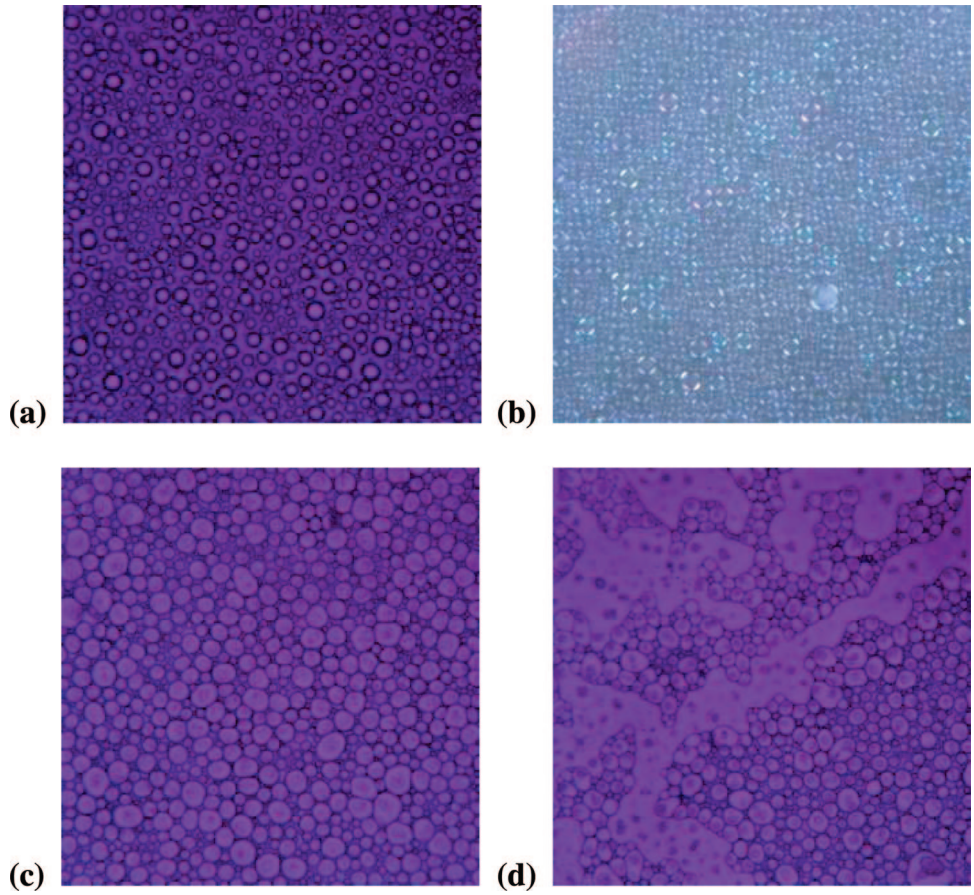

Figure 7. Thermal behavior of ritonavir mesophase precipitated onto a glass coverslip at pH 3 and heated at 10 °C/min from (a) −20 to 25 °C, and (b) maintained birefringence as seen with the aid of a λ-plate. Heating to (c) 50 °C causes dehydration of the mesophase which results in swelling and porous surfaces. Heating to (d) 70 °C leads to coalescing of the mesophase and formation of an isotropic phase.

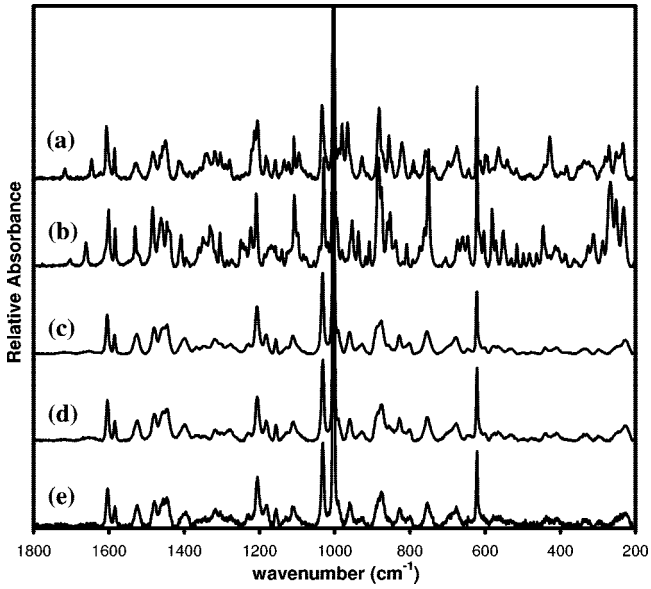

Figure 8. Comparison of the Raman spectra of ritonavir (a) crystalline Form I, (b) crystalline Form II, (c) amorphous phase prepared by quench cooling the melt, (d) mesophase precipitated at pH 3, and (e) mesophase precipitated at pH 7.

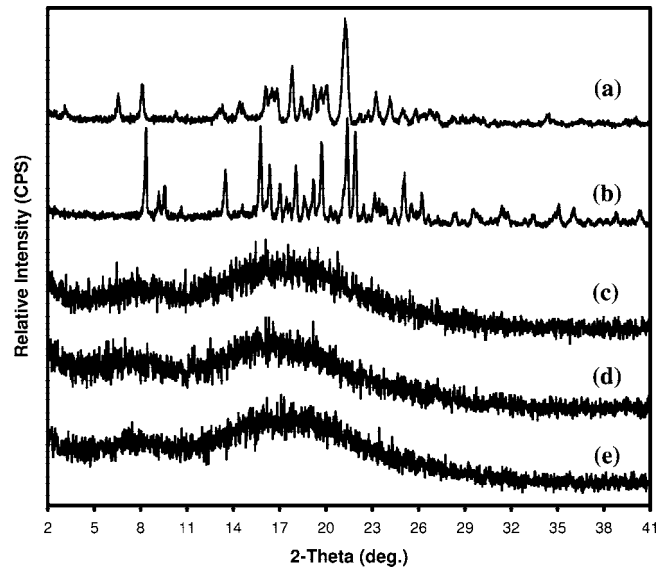

Figure 9. XRPD comparing ritonavir solid phases: (a) crystalline Form I, (b) crystalline Form II, (c) amorphous phase prepared by quench cooling the melt, (d) mesophase following precipitation at pH 3, and (e) mesophase following precipitation at pH 7.

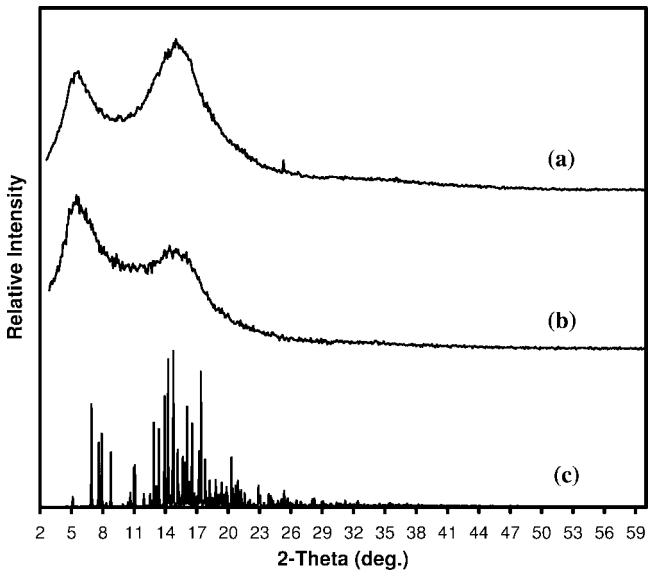

Figure 10. Synchrotron X-ray powder diffraction of (a) mesophase precipitated at pH 3, (b) amorphous ritonavir, and (c) crystalline Form II.

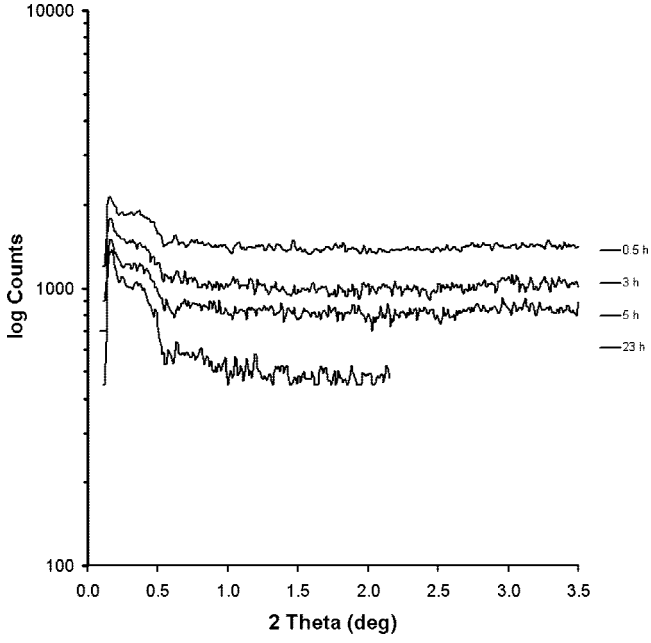

Figure 11. Small-angle X-ray scattering during ritonavir mesophase precipitation at pH 3 monitored up to 23 h.

the surface tension (γ) of RTV over a range of solution concentrations (0−0.455 mM) at 25 °C. Lyotropic liquid crystals formed by molecular associations in solution may also exhibit high surface activity. Since an iridescent surface film (Figure 3a) formed at the air/water interface following pH-induced RTV precipitation, surface activity was suspected. Results show that RTV lowered the surface tension of aqueous solutions (Table 1). The surface tension of 0.455 mM RTV was 57.6 compared to 71.7 dyn/cm without RTV. RTV is surface active even at low concentrations of 0.0139 mM in pH 3 buffer and 0.00139 mM in pH 7 buffer, such that γ decreases to 51.5 and 51.7 dyn/cm, respectively. The

Table 1. Surface Tension of Ritonavir Solutions (25°C)

solution	[RTV] (mM)	γ (dyn/cm)[a]
water	0	70.6 ± 0.6
pH 1 phosphate buffer	0	71.7 ± 0.2
pH 3 phosphate buffer	0	72.6 ± 0.1
pH 7 phosphate buffer	0	71.4 ± 0.1
pH 1 phosphate buffer	0.455	57.6 ± 0.1
pH 3 phosphate buffer	~0.0139	51.5 ± 0.2
pH 7 phosphate buffer	~0.00139	51.7 ± 0.5

[a] Values are expressed as the average (n = 5) with standard deviation.

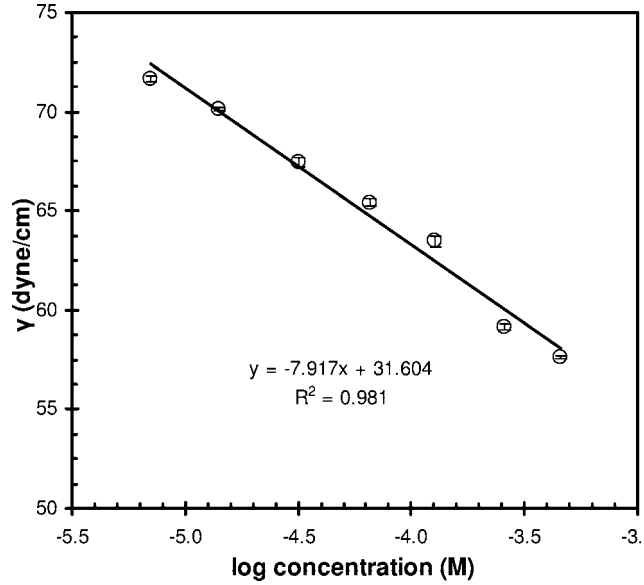

Figure 12. Surface tension of ritonavir solutions as a function of concentration measured at pH 1 and 25 °C.

surface activity of RTV confirms that it self-assembles in aqueous solution, thus forming the mesophase structure.

The RTV surface excess was measured from the limiting slope below the critical micelle concentration (CMC) (Figure 12). Although the CMC was not determined because the preparation of highly concentrated solutions was limited by RTV's low aqueous solubility, surface excess calculations provide practical insight into the self-association behavior of RTV. Surface excess concentrations (Γ) can be determined from the Gibbs equation:

$$\Gamma = -\left(\frac{1}{2.303RT}\right)\left(\frac{\partial\gamma}{\partial \log c}\right) \quad (1)$$

The surface excess measured at pH 1 and 25 °C is 1.39×10^{-3} mol/m^2. The surface area occupied per molecule was determined to be 0.00120 nm^2 from the surface excess using the relation:

$$A = 1/(N_A\Gamma) \quad (2)$$

where A is the surface area and N_A is Avogadro's number. The surface excess is known to be affected mostly by the size of the hydrophilic portion of amphiphilic molecules, such as surfactants.[26,27]

Dissolution Rate. The solubilities of the RTV mesophase, amorphous solid, and crystal Form I were estimated from

Table 2. Dissolution Rates and Solubilities of Ritonavir Phases at pH 1 (25°C)

initial solid phase	initial dissolution rate ($\mu g \cdot cm^{-2} min^{-1}$)[a]	solubility (mg/g)[a]
Form II	10.089 ± 0.002	0.192 ± 0.002
Form I	21.376 ± 0.002	0.407 ± 0.002
mesophase	204.433 ± 0.006	3.893 ± 0.006
amorphous	226.675 ± 0.008	4.317 ± 0.008

[a] Values are expressed as an average (n = 3) with standard deviation.

the initial disk dissolution rates of each phase, from the dissolution rate of crystal Form II, and from the previously measured equilibrium solubility of Form II according to the method of Shefter and Higuchi:[28]

$$S_X = \frac{(dC/dt)_X}{(dC/dt)_{\text{Form II}}} S_{\text{Form II}} \quad (3)$$

S_X is the solubility of either Form I, mesophase, or amorphous RTV, $S_{\text{Form II}}$ is the equilibrium solubility of crystal Form II, and $(dC/dt)_X$ and $(dC/dt)_{\text{Form II}}$ are the initial dissolution rates of the desired phase and Form II, respectively. This expression is valid when dissolution is diffusion-controlled, which has been shown for RTV.[14]

The dissolution rates and aqueous solubilities of RTV phases in 0.1 N HCl at 25 °C are listed in Table 2. The aqueous dissolution and solubilities of each phase are consistent with the degree of order in the structures. The most thermodynamically stable phase will generally have the greatest degree of order. Therefore, the most stable phase (Form II) will be less soluble and have a slower dissolution rate than that of the least thermodynamically stable phase (amorphous). As expected, the relative dissolution rates and solubilities can be ranked: amorphous > mesophase ≫ Form I > Form II. The difference in dissolution and solubility between Form I and Form II is 2-fold, whereas the less ordered phases (mesophase and amorphous) are approximately 10-fold higher than that of Form I and 20-fold higher than that of Form II. Law et al.[14] have also reported a 10-fold difference between the dissolution rates of amorphous RTV and Form I at 37 °C in 0.1 N HCl. The dissolution rates and solubilities of the mesophase and amorphous RTV have been confirmed to be statistically different, based on their 95% confidence limits.

At the conclusion of the dissolution studies for amorphous RTV (30 min), the disk surfaces showed vesicles very similar to those of the mesophase. Additional studies were designed to determine whether the amorphous phase of RTV is stabilized by the formation of the mesophase when exposed to aqueous environments.

Transformation of Amorphous RTV in Suspension. Amorphous RTV when suspended in water and in 0.3 M phosphate buffer (pH 3 and 7) at room temperature (22 °C) generates spherical vesicles on its surface (Figure 13a) that transform to Form I within 3 days (Figure 13b). Phase transformation proceeds as the amorphous and mesophases dissolve (within 30 days, Figure 13c). Conversion to the more thermodynamically stable Form II was not observed over the course of this study (1 month).

The mesophase generated during dissolution of the amorphous phase exhibited spectral differences from those of the amorphous phase (Figure 14). The spectral differences observed from 1200 to 1500 cm^{-1} may be the result of different molecular interactions in the mesophase structure in water. It is unlikely that the spectral peaks in this region are a contribution of water alone, since Raman is not sensitive to water and the other solid phases of RTV do not show these peaks when dispersed in water.

Discussion

Given the low pK_a, low intrinsic aqueous solubility, and high oral dose of the weak base HIV protease inhibitors, precipitation from supersaturated solution in the small intestine following emptying of dissolved drug from the stomach might be anticipated. For RTV, the possibility that a different polymorphic form might be generated under these conditions was considered based on drug formulation issues.[12,13] Our results show that RTV self-assembles into nanovesicles by raising the pH of aqueous solutions. These vesicles grow to the macroscale and transform to crystal Form I and subsequently to Form II, the stable crystal polymorph.

The phase resulting from pH-induced precipitation was initially suspected to be amorphous based on X-ray diffraction and DSC studies. Amorphous solids lack long-range order, are isotropic, and are not birefringent.[29] However, the birefringence observed by POM combined with SAXS and synchrotron X-ray diffraction indicate orientational order associated with nematic lyotropic liquid crystalline phases which have orientational order but no positional order.[30,31] Whereas crystals exhibit three-dimensional short and long-range order, mesophases differ in the extent of positional, orientational, and conformational order. Most exhibit one or two-dimensional long-range order and may possess short-range order. Lamellar liquid crystals have one-dimensional

(26) Attwood, D.; Florence, A. T. *Surfactant Systems. Their Chemistry, Pharmacy and Biology*; Chapman and Hall: New York, 1983.

(27) Treguier, J. P.; Lo, I.; Seiller, M.; Puisieux, F. Emulsions and diagrams of water-surfactant-oil systems-study on water-brij92(96)-vaseline system-influence of hydrophilic properties of surfactant. *Pharm. Acta Helv.* **1975**, *50* (12), 421–431.

(28) Shefter, E.; Higuchi, T. Dissolution behavior of crystalline solvated and nonsolvated forms of some pharmaceuticals. *J. Pharm. Sci.* **1963**, *52* (8), 781–791.

(29) Shalaev, E.; Zografi, G. The concept of 'structure' in amorphous solids from the perspective of the pharmaceutical sciences In *Amorphous Food and Pharmaceutical Systems*; The Royal Society of Chemistry: Cambridge, 2002.

(30) Mueller-Goymann, C. C. Drug Delivery - Liquid Crystals. In *Encyclopedia of Pharmaceutical Technology*; Marcel Dekker, Inc.: New York, 2002.

(31) Wunderlich, B. A classification of molecules, phases, and transitions as recognized by thermal analysis. *Thermochim. Acta* **1999**, *341*, 37–52.

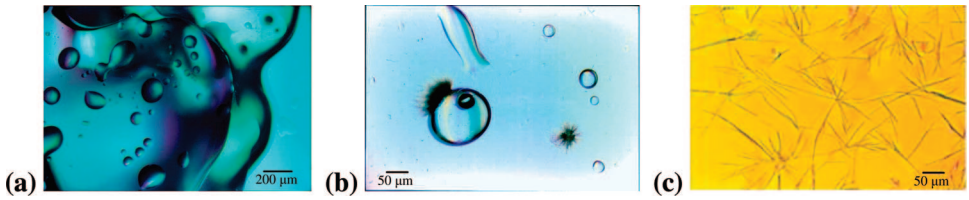

Figure 13. Phase separation and crystallization from amorphous ritonavir dispersed in aqueous solution (water, 22 °C). Amorphous surface (a) undergoes a phase separation to vesicles at $t = 24$ h, (b) mesophase is depleted along with solvent-mediated phase transformation to Form I at $t = 3$ days, and (c) phase transformation to Form I is complete within 30 days.

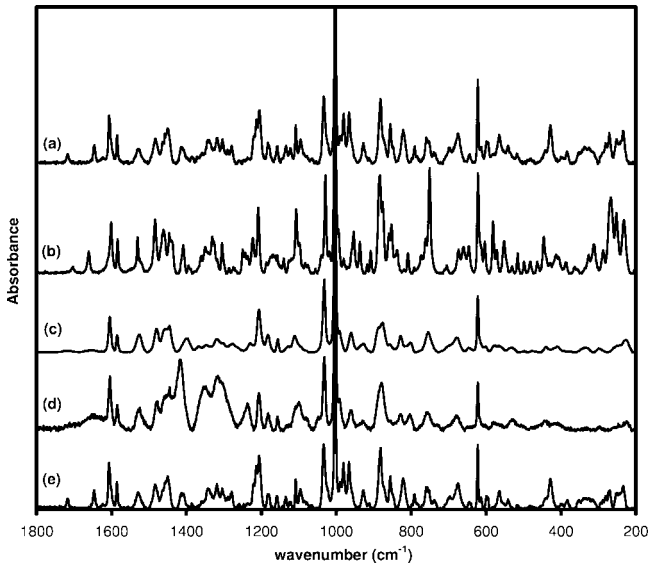

Figure 14. Raman spectra showing changes of amorphous ritonavir dispersed in water at 22 °C. Comparison of (a) crystalline Form I, (b) crystalline Form II, (c) amorphous before dispersion in water, (d) amorphous dispersed in water after 24 h, and (e) amorphous dispersed in water after 3 days.

positional order. Nematic liquid crystals lack positional and conformational long-range order but maintain some degree of orientational long-range order and may exhibit short-range order. The orientational order of molecules in liquid crystals gives rise to their characteristic birefringence.

Liquid crystals are common in pharmaceutical systems. Some drug molecules are able to form liquid crystals either alone or with solvent and are classified as thermotropic and lyotropic liquid crystals, respectively.[30,32] Thermotropic liquid crystals are formed with an increase in temperature that results in thermal motions of the molecules. When molecular mobility and order are introduced in the presence of solvent, a lyotropic liquid crystal is formed. Formation of this phase is solvent- and concentration-dependent. As RTV mesophase formation was observed in aqueous solutions of concentration >30 μg/g under isothermal conditions, the mesophase is likely to be a lyotropic liquid crystal.

Since liquid crystals and other mesophases may appear amorphous when characterized by the more common techniques of XRPD and DSC, the literature may not accurately reflect the number of pharmaceutically relevant compounds that form liquid crystals. It has been estimated that one in every 200 molecules synthesized possess a liquid crystalline phase.[32] To distinguish between these phases, high-resolution diffraction techniques such as synchrotron X-ray and small-angle X-ray scattering (SAXS) may be used. These techniques can detect the long-range order characteristic of liquid crystals that may otherwise go undetected by XRPD. The two-dimensional liquid crystal phase of spray-dried cyclosporine, for example, was identified using SAXS and POM data.[18] Cyclosporine may have been incorrectly classified as amorphous due to the lack of diffraction peaks by XRPD and T_g-like events by DSC.[18]

A number of pharmaceutically and physiologically relevant liquid crystals have been described in the literature. Drug substances known to form thermotropic and/or lyotropic liquid crystals include cyclosporine,[18,33] itraconazole,[34] cromolyn sodium,[35,36] amiodarone,[37] and several nonsteroidal anti-inflammatory drugs (NSAIDs) such as ibuprofen, fenoprofen, ketoprofen, and flurbiprofen.[38,39] Surfactants, peptides, proteins, and polymers represent a diverse array of

(32) Collings, P. J. *Liquid crystals: nature's delicate phase of matter*; Princeton University Press: Princeton, NJ, 2002.

(33) Stevenson, C. L.; Tan, M. M.; Lechuga-Ballesteros, D. Secondary structure of cyclosporine in a spray-dried liquid crystal by FTIR. *J. Pharm. Sci.* **2003**, *92* (9), 1832–1843.

(34) Six, K.; Verreck, G.; Peeters, J.; Binnemans, K.; Berghmans, H.; Augustijns, P.; Kinget, R.; Van den Mooter, G. Investigation of thermal properties of glassy itraconazole: identification of a monotropic mesophase. *Thermochim. Acta* **2001**, *376* (2), 175–181.

(35) Hartshorne, N. H.; Woodard, G. D. Mesomorphism in system disodium cromoglycate-water. *Mol. Cryst. Liq. Cryst.* **1973**, *23* (3−4), 343–368.

(36) Chen, L. R.; Young, V. G.; Lechuga-Ballesteros, D.; Grant, D. J. W. Solid state behavior of cromolyn sodium hydrates. *J. Pharm. Sci.* **1999**, *88* (11), 1191–1200.

(37) Bouligand, Y.; Boury, F.; Devoisselle, J. M.; Fortune, R.; Gautier, J. C.; Girard, D.; Maillol, H.; Proust, J. E. Liquid crystals and colloids in water-amiodarone systems. *Langmuir* **1998**, *14* (2), 542–546.

(38) Hamann, H. J.; Mueller-Goymann, C. C. Lyotroper Mesomorphismus von Arzneistoffmolekulen Unter Besonderer /berucksichtigung der Profene. *Acta Pharm. Technol.* **1987**, *33*, 67–73.

(39) Rades, T.; Mueller-Goymann, C. C. Melting Behavior and Thermotropic Mesomorphism of Fenoprofen Salts. *Eur. J. Pharm. Biopharm* **1994**, *40*, 277–282.

(40) Giorgi, T.; Grepioni, F.; Manet, I.; Mariani, P.; Masiero, S.; Mezzina, E.; Pieraccini, S.; Saturni, L.; Spada, G. P.; Gottarelli, G. Gel-like lyomesophases formed in organic solvents by self-assembled guanine ribbons. *Chem.—Eur. J.* **2002**, *8* (9), 2143–2152.

structures also known to form liquid crystals.[15,17,19] For instance, bile salts, cellulose derivatives, phospholipids, and double helical polynucleic acids are biologically important molecules which form lyotropic liquid crystals at high enough concentrations in water.[32] The ability of these molecules to form highly ordered structures in water provides a delicate balance between rigidity and fluidity essential to biological function. Pharmaceutically relevant liquid crystals provide an opportunity for modulating drug release and because of their disordered structure may enhance aqueous solubility and dissolution rates relative to the crystalline state.

Law et al.[14] have reported that amorphous RTV formed a gelatinous mass at the conclusion of dissolution studies in 0.1 N HCl at 37 °C. Gel-like phases are commonly observed for compounds that form lyotropic liquid crystals, as in the case of the drug amiodarone[37] and lipophilic guanosine derivatives.[40] It is therefore possible that amorphous RTV transforms to a lyotropic liquid crystalline phase in aqueous environments.

Conclusion

RTV molecules self-assemble to form nanostructures when high supersaturation is generated by changing pH. This phase has the mobility and order characteristic of a lyotropic liquid crystal and leads to enhanced dissolution and solubility. Thus, nano- to macroscale liquid crystal formation induced by increasing pH, as in the small intestine subsequent to gastric emptying, has the potential to increase the absorption of poorly soluble drugs.

Acknowledgment. We are grateful to Prof. John Bilello from the University of Michigan, Materials Science Department, for synchrotron X-ray diffraction analysis. We acknowledge financial support from the American Foundation for Pharmaceutical Education, U.S. Pharmacopeia, National Consortium for Graduate Degrees for Minorities in Engineering and Science, Inc., Purdue−Michigan Consortium on Supramolecular Assemblies and Solid State Properties, and Fred W. Lyons, Jr. Fellowship and Lilly Endowment Fellowship both from The University of Michigan College of Pharmacy. Abbott Laboratories, North Chicago, IL, is acknowledged for their donation of ritonavir.

MP800114K